Author Manuscript

Author Manuscript

Author Manuscript

Author Manuscript

HHS Public Access

Author manuscript

Biomed Pharmacother. Author manuscript; available in PMC 2019 May 16.

Published in final edited form as:

Biomed Pharmacother. 2017 August ; 92: 394–402. doi:10.1016/j.biopha.2017.05.093.

Antiangiogenic activity of PLGA-Lupeol implants for potential intravitreal applications

Daniel Crístian Ferreira Soares[a,*], **Diogo Coelho de Paula Oliveira**[b], **Luciola Silva Barcelos**[c], **Alan Sales Barbosa**[c], **Lorena Carla Vieira**[b], **Danyelle M. Townsend**[d], **Domenico Rubello**[e], **André Luis Branco de Barros**[f,*], **Lucienir Pains Duarte**[g], and **Armando Silva-Cunha**[b]

[a]Universidade Federal de Itajubá, Itabira, Minas Gerais, Brazil

[b]Department of Pharmaceutical Products, Faculty of Pharmacy, Universidade Federal de Minas Gerais, Belo Horizonte, Minas Gerais, Brazil

[c]Department of Physiology and Biophysics, Institute of Biological Sciences, Universidade Federal de Minas Gerais, Belo Horizonte, Minas Gerais, Brazil

[d]Department of Drug Discovery and Pharmaceutical Sciences, Medical University of South Carolina, United States

[e]Department of Nuclear Medicine, Imaging and Clinical Pathology, Santa Maria della Misericordia Hospital, Rovigo, Italy

[f]Department of Clinical and Toxicological Analyses, Faculty of Pharmacy, Universidade Federal de Minas Gerais, Belo Horizonte, Minas Gerais, Brazil

[g]Department of Chemistry, Universidade Federal de Minas Gerais, Belo Horizonte, Minas Gerais, Brazil

Abstract

Uncontrolled angiogenesis is directly associated with ocular diseases such as macular degeneration and diabetic retinopathy. Implantable polymeric drug delivery systems have been proposed for intravitreal applications and in the present work, we evaluated the antiangiogenic potential of PLGA ocular implants loaded with the triterpene lupeol using *in vitro* and *in vivo* models. The drug/polymer physiochemical properties of the lupeol-loaded PLGA were validated as functionally similar using differential scanning calorimetry, Fourier transform infrared spectroscopy, and scanning electron microscopy. Interestingly, in an *in vitro* culture system, lupeol (100 μg/mL and 250 μg/mL) was capable to inhibited the proliferation as well as the migration of Human Umbilical Vein Endothelial Cells (HUVEC), without interfering in cell viability, promoting a significant reduction in the percentage of vessels (39.41% and 44.12%, respectively), compared with the control group. *In vivo* test, by using the chorioallantoic membrane (CAM) model, lupeol-loaded PLGA ocular implants showed antiangiogenic activity comparable to the

[*]Corresponding authors. soares@unifei.edu.br (D.C.F. Soares), brancodebarros@yahoo.com.br (A.L.B. de Barros).

Appendix A. Supplementary data

Supplementary data associated with this article can be found, in the online version, at http://dx.doi.org/10.1016/j.biopha.2017.05.093.

Author Manuscript Author Manuscript Author Manuscript Author Manuscript

FDA-approved anti-VEGF antibody Bevacizumab. Overall, our results suggest lupeol-loaded PLGA ocular implants were able to inhibit the angiogenic process by impairing both proliferation and migration of endothelial cells.

Keywords

Lupeol; Antiangiogenic activity; Intravitreal assays; PLGA ocular implants

1. Introduction

Angiogenesis is a natural process that occurs in the human body during fetal development or as a response to tissue damage, as part of wound healing process and renewing the blood flux in damage areas [1,2]. When the human body loses its capacity to maintain adequately the equilibrium of angiogenic mediators, some diseases can develop, including arthritis, cancer, endometriosis, psoriasis, macular degeneration related to age and proliferative diabetic retinopathy [3,4]. Macular degeneration related to age is the main cause of blindness in persons older than 60 years in industrialized countries [5]. The prevalence of blindness can vary between 10 and 15% among affected persons and estimates have shown a significantly rates increase until 2030 [6]. Currently, available treatments are limited to palliatives such as photodynamic therapy, intravitreal injections with corticoids, antiangiogenic compounds applied directly into eye and laser photocoagulation [7–10]. The proliferative diabetic retinopathy is characterized by new important vascularization in retina, following to intravitreal interface, with possible loses of normal visual characteristics mainly due to traditional retinal detachment. In this sense, the inhibition of angiogenesis can be considered an important strategy to treat these intraocular diseases and have been explored in many published works [11–14].

Lupeol is a natural pentaciclic triterpene with a lupane scaffold that can be found in diverse vegetables, including white cabbage, red pepper, cucumber, tomatoes, carrots, peas, and soy. Moreover, administration of lupeol does not result in systemic toxicity in animal models in doses ranging from 30 to 2000 mg kg^{-1} [15]. Triterpene can be isolated from medicinal plants, *i.e. Celastraceae* family plants, displaying clinically relevant biological properties related to inflammation, arthritis, cardiovascular disorders, cancer and wound healing processes [16–18]. You et al. [19] evaluated the antiangiogenic activity of lupeol on a tube-like formation assay using HUVEC cells (*Human umbilical vein endothelial cells*). The results revealed lupeol capacity to inhibit 80% of angiogenic processes at a non-toxic dose of 50 μgmL^{-1}, whereas lower doses showed a significant reduction in antiangiogenic activity reaching only 40% of initial values. Other studies using an endothelial cell model have indicated that triterpenes can modulate growth factors such VEGF (Vascular endothelial growth factor) and are capable of inducing cellular differentiation, seeking to inhibit the vascular tissue growth, displaying an important antiangiogenic effect [20–23].

Due to anatomical and physiologic characteristics of the eye, administration of ophthalmic medicines is difficult and many studies showed that only approximately 5% of the administrated dose are absorbed by intraocular tissues, making the treatment unfeasible for

Author Manuscript Author Manuscript Author Manuscript Author Manuscript

diseases located in posterior segment of the eye. Other available treatments require the use of high drug doses or are too invasive as intravitreal injections, exhibiting great risks and potentially serious side effects to the patient [24–26]. Seeking to overcome this negative scenario, research has been dedicated to developing new drug delivery systems, such as polymeric implants with the overall goal to be more selective and achieve favorable bioavailability profiles through sustained releasing of the therapeutic cargo [27,28]. Such systems offer many advantages, including favorable patient compliance, biocompatibility, predictable biodegradation kinetic and mechanical resistance in various intravitreal applications [29–31]. In order to mitigate the cumulative risks associated with repeated intravitreal injections, some implantable polymeric systems have been approved by FDA and currently available, for example: Ozurdex® (Dexamethasone Intravitreal Implant); Iluvien® (Fluocinolone acetonide intravitreal implant) and Triesence® (Triamcinolone acetonide). In these systems, any cytotoxicity was observed as well as significant antiangiogenic activity were obtained, displaying the applicability of these systems in intravitreal applications. However, at present, no steroid has achieved US FDA approval for the treatment of pathologies associated to angiogenesis (except for ranibizumab, a monoclonal antibody).

In this work, we aimed to evaluate the anti-angiogenesis activity of PLGA ocular implants containing the lupeol, a non-steroid compound, in both *in vitro* and *in vivo* models.

2. Experimental

2.1. Chemical and reagents

Poly (D,L-lactide-co-glycolide) in ratio of 75:25 [PLGA (75:25)] was purchased from Boehringer Ingelheim (Germany). All the solvents and reagents used in buffer solutions, in the preparation of the implants, and mobile phase were HPLC or analytical grade. Water was distilled, deionized and filtered through a 0.22 mm filter (Millipore, USA).

2.2. Methods

2.2.1. Lupeol extraction—Dried and pulverized stem of *Maytenus salicifolia* (2525.9 g) were subjected to exhaustive maceration in *n*-hexane at room temperature, yielding 14.7 g of hexane extract. It was subjected to silica gel column chromatography (CC) eluted with *n-hexane*, $CHCl_3$, AcOEt, and MeOH, pure or in mixtures of enhanced polarity, yielding 52 fractions gathered in 14 groups. Group 8 (Fraction 31; 137 mg) was chromatographed on silica gel CC eluted with *n*-hexene/$CHCl_3$ (4:1) furnishing 25 fractions of 5 mL each. Fractions 5–12 providing a white solid (93.0 mg) which was identified as lupeol. The structural elucidation of this compound was based on its IR, ^{1}H and ^{13}C NMR spectral data.

2.2.2. Lupeol characterization—Lupeol was characterized by melting point, FTIR and NMR spectra. Melting point was uncorrected and measured using Thermo system FP800 Metler apparatus. FTIR spectrum were recorded on a Perkin-Elmer, FTIR Spectrum-1000 and NMR experiments were carried out on Bruker DRX400 Avance 3 spectrometer, using TMS as an internal standard and CDCl as solvent.

Author Manuscript Author Manuscript Author Manuscript Author Manuscript

2.2.3. PLGA-lupeol implant preparation—Lupeol-loaded PLGA ocular implants were prepared according to method developed by Fialho and da Silva [32]. Briefly, 100 mg of PLGA 75:25 and 30 mg of lupeol were dissolved in 10 mL of acetone at room temperature. Then, the solution was placed in a freezer under −80 °C. Afterwards, the frozen solution was lyophilized for 30 h and the obtained material were then molded to rods using Teflon® sheets heated on a hot plate from 50 to 60 °C in order to form lupeol-loaded PLGA ocular implants with diameter of 0.45 mm and length of 6 mm, containing 30% lupeol w/w.

2.2.4. Physicochemical characterization

2.2.4.1. Differential scanning calorimetry (DSC).: Differential scanning calorimetry analysis (DSC) DSC-50, Shimatzu DSC apparatus was used. The samples constituted by lupeol; blank PLGA 75:25 and lupeol-loaded PLGA ocular implants were heated in semi-hermetic aluminum pans, and the first scan was measured at a heating rate of 10°C min^{-1} from room temperature to 180 °C. Subsequently, the samples were cooled t −100 °C and heated to 400 °C (second run) under nitrogen atmosphere.

2.2.4.2. Fourier transform infrared spectroscopy (FTIR).: Fourier transform infrared spectroscopy (FTIR) Infrared spectra were collected in a Fourier transform infrared spectrophotometer (FTIR) (model Spectrum 1000; Perkin Elmer). Measurements were carried out using the attenuated total reflectance (ATR) technique. Each spectrum was a result of 32 scans with a resolution of 4 cm^{-1}, between ranging 4000–650 cm^{-1}. Samples were constituted by lupeol; blank PLGA 75:25 and lupeol-loaded PLGA ocular implants.

2.2.5. Morphological characterization—The structure of lupeol-loaded PLGA ocular implants was observed by scanning electron microscope TESCAN VEGA 3 LMU (Czech Republic). Samples characterized by 4 mm of length and 0.5 mm of diameter were gold-coated and imaging were conducted in voltage of 10 kV.

2.2.6. In vitro *antiangiogenic studies*

2.2.6.1. HUVEC cells culture and cytotoxicity evaluation.: Human Umbilical Vein Endothelial Cells (HUVEC; ATCC – CRL-2873) were cultured in endothelial cell supplemented media (Endothelial Growth Medium, EGM-2; Lonza). Cells in the sixth or seventh passage were used in the experiments after incubation in deprivation medium (Endothelial Basal Medium, EBM-2; Lonza) containing 0.1% fetal bovine serum (FBS) overnight at 37 C 5% CO_2, for cell cycle synchronization.

Lupeol was initially diluted in phosphate-buffered saline (PBS) containing 10% dimethyl sulfoxide (DMSO), and 10mg mL^{-1} stock solutions were aliquoted and frozen. For cell treatment, lupeol stock solution was diluted in EBM-2 10% FBS to the experimental doses tested (10, 30 and 100 μm mL^{-1}) and cells were exposed to no more than 0.1% DMSO.

Two different protocols were applied to evaluate both cell viability and proliferation: Trypan Blue and Presto Blue assays. For the Trypan Blue assay, after cell cycle synchronization, HUVEC were treated with lupeol or vehicle and cultured in 24 well plates for 48 h. At the end of this period, cells were trypsinized, stained with Trypan Blue and both viable and non-

Author Manuscript Author Manuscript Author Manuscript Author Manuscript

viable (blue) cells were counted using a Neubauer chamber. For the Presto Blue assay, cells were cultured in 96 well plates and, after cell cycle synchronization, treated with lupeol or vehicle. Presto Blue was added 2 h before first fluorescence reading, according to manufacturer instructions for the kit used (ThermoFisher).

2.2.7. Migration assay—In order to evaluate the effects of lupeol on the migration of endothelial cells, the scratch wound assay was performed as described by [33]. HUVEC were seeded in 48 well plates and, after overnight deprivation, a single scratch was made on the cell monolayer using a sterile pipette tip. Each well was washed with PBS for removal of scrapped cells and 2 mM hydroxyl urea was added, preventing cell proliferation and allowing the observation of the exclusive role of migration on open area closure. Cells were treated with lupeol in different concentrations (10, 30, and 100 mg/ mL) or vehicle immediately after scratching and incubated for 36 h. The cell monolayer was imaged at both the beginning and the end of this period using a camera attached to an inverted microscope. TScratch software (CSELab, Zurich) was used for open area measurement and migration quantification.

2.2.8. In vivo *antiangiogenic studies*

2.2.8.1. Chorioallantoic membrane assay.: Chorioallantoic membrane (CAM) model was used to evaluate the *in vivo* antiangiogenic activity of 20 μL of lupeol in different concentrations (100 μg/mL and 250 μg/mL) and biodegradable implants containing or not containing lupeol. The negative control was 20 μL of phosphate-buffered-saline (PBS, pH 7.4) and the positive control was 20 mL of bevacizumab solution at 250 μg/mL (Avastin®, Produtos Roche Químicos e Farmacêuticos S.A., Brazil). First, 20 fertilized chicken eggs per group were transferred into a hatching incubator (Premium Ecologica, Brazil) with 60% of relative humidity and temperature fixed at 37 C. On day three of embryonic development, a circular opening about 1.0 cm in diameter in the region of the air chamber of the eggshell was made, and the inner shell membrane was removed to expose the CAM. On day five, samples were applied over the CAM in a predetermined site. On the 7th day of incubation, the CAMs were extracted after previous fixation with a formaldehyde solution of 3.7% for 10 min, and analyzed with a stereomicroscope (Leica, model DM4000B, Germany) coupled to a Leica digital CCD camera model DFC 280 (Software Leica Application Suite V 3.3.0, Germany). The obtained images were processed with the program Image J (version 1.44p; National Institutes of Health, USA) and the control group was set to 100% for blood vessels quantification.

3. Statistical analysis

The mean values and standard deviation were calculated. The statistical parameters were analyzed through ANOVA followed post-test of Tukey or Bonferroni where p 0.05 was considered as statistically significant. The Mann–Whitney non-parametric test was used to compare outcomes in both groups. The unpaired-test was used to compare outcomes of percent blood vessels in the CAM study. Values of $p \leq 0.05$ were considered to be statistically significant. Interrelation between dark-adapted b-wave amplitude and stimuli luminance was modeled using the Naka–Rushton function that yields the parameters: Vmax

Author Manuscript Author Manuscript Author Manuscript Author Manuscript

asymptotic (maximum b-wave amplitude) the light he necessary luminance reaching 50% of Vmax, which is a mark of dark-adapted sensitivity; and is the dynamic working range of photoreceptors.

4. Results and discussion

4.1. Lupeol characterization

Lupeol was obtained as a white solid and its molecular structure are presented in Fig. 1. The IR spectrum of Lupeol presented absorption bands at 3313 cm^1 (OH),1638 (C=C) and 878 (=CH). ^{13}The C NMR spectral data were similar to the one related by Kundu [34].

4.2. Physicochemical characterization

4.2.1. Differential scanning calorimetry (DSC)—DSC curves for lupeol, blank PLGA 75:25 and lupeol-loaded PLGA ocular implants are presented in Fig. 2 (respectively A–C). Lupeol presented during the heating two important peaks that were correlated to phase transitions and melting point. According to Macêdo et al. [35] the first peak, at 187.11 C, can be attributed to molecular arrangement occurring in the chiral centers of the molecule and the second peak, at 212.38C can be related to the melting point of substance.

For blank PLGA 75:25 samples, the DSC analysis showed that endothermic reactions were identified at 56.7C referring to glass transition of polymer. Events observed between 290 and 330C were attributed to thermal decomposition of polymer. A peak related to melting point was not observed due to amorphous characteristic of polymer. All the values encountered are consistent and in accordance with prior characterization by Mainardes et al. [36].

Lupeol-loaded PLGA ocular implants showed in the DSC curve endothermic process at 57.81 C referring to glass transition of polymer already determined. Following the same behavior, at 183.65 C was observed a peak already attributed to molecular arrangement of polymer. Any other significant peak was observed in these samples, supporting that lupeol and PLGA likely has only physical interactions and no significant molecular changes or interactions occurred. This can be considered an important feature, since lupeol can be released from polymeric matrix without any modification, preserving thus intact the lupeol molecular structure.

4.2.2. Fourier transform infrared spectroscopy (FTIR)—FTIR was used to evaluate possible chemical interactions between lupeol and PLGA chains or possible modifications in the original molecules that can conduct to lost in biological activity. Three different samples groups (lupeol; blank PLGA 75:25 and lupeol-loaded PLGA ocular implants). The FTIR spectrum of sample constituted by physical mixture between lupeol and PLGA (lupeol-loaded PLGA ocular implants) is shown in Fig. 3.

The FTIR spectrum of blank PLGA 75:25 (data not shown) presented a characteristic band at 1749 cm^{-1} attributed to carbonyl stretching of ester groups. Methyl groups were identified by absorption band at 2995 cm^{-1} attributed to C—H bonds. Events related to C—O and O—H stretching are observed in 1452 and 1000 cm^{-1}, respectively. All main peaks were confirming with data published by Yang et al. [37]. Lupeol-loaded PLGA implant samples

Author Manuscript Author Manuscript Author Manuscript Author Manuscript

presented bands at 3279 and 2946 cm^{-1} attributed to O—H and C—H bonds. An intense band at 1087 cm^{-1} was attributed to superposition bands of asymmetric stretching of C=C bond of lupeol and C—H bonds of PLGA methyl groups. We did not observe new bands in lupeol-loaded PLGA ocular implants FTIR spectrum (Fig. 3), thus we concluded the structures of the both compounds were maintained stable and no effective chemical bonds occurred between them, in agreement with the results encountered in thermal analysis.

4.3. Morphological characterization

Lupeol loaded- PLGA ocular implants were evaluated using Scanning Electron Microscopy, Fig. 4. Micrographs revealed cylinders with approximately 4.5 cm of length with homogeneous surface and absence of significant superficial irregularities with magnification of 100× (a) and 30× (b). In image C (500× magnification) it was possible to identify slight superficial roughness and pores probably formed during molding process of polymer. Furthermore, in all studied magnifications the implant images presented heterogeneous shades of gray, corresponding to different electrons number detected, that can be correlated to the structural information and the density. For example, pores appear dark, reflecting lower electrons yields. On the other hand, brighter gray can reflect more high density in the structure. However, the different shades of gray cannot be used to confirm the physical lupeol distribution in implant.

4.4. In vitro *antiangiogenic studies*

4.4.1. HUVEC cells culture and cytotoxicity evaluation—To confirm that lupeol exhibited antiangiogenic properties, *in vitro* and *in vivo* approaches were applied. The antiangiogenic properties were briefly reported by You et al. [19] using a tube-like formation assay. Vessel formation is known to be driven by two basic endothelial cell activities, proliferation and migration, which provide information on the mechanisms by which angiogenesis is being promoted or repressed. We observed a significant decrease of approximately 40% in cell proliferation after treatment with 100 μg/mL of Lupeol when compared to the EBM-2 10% FBS control. This effect was not found at lower concentrations, which resulted in a non-significant decrease of approximately 20% in cell counts after treatment with 10 or 30 μg/mL of Lupeol (Fig. 5). It is confirmed when the final number of cells is normalized by the initial number seeded *per* well, providing a percentage of proliferation.

These results suggest a higher concentration of lupeol is needed to disrupt proliferative effects of growth factors, similarly to how other triterpenes seem to act [20], as the ones present in FBS, namely VEGF [38]. This disruption seems to occur by inhibition of multiple targets in β-catenin signaling [39]. Furthermore, *in silico* analysis also suggest lupeol is able to bind VEGFR2, revealing this as a possible additional mechanism [40].

As cytotoxic effects of the drug might also influence cell number after treatment, HUVEC viability was evaluated after exposure to lupeol. In the Trypan Blue assay, cells which incorporated the reagent and, therefore, are believed to present cell membrane damage (since Trypan Blue is not permeable to it) were considered non-viable. No statistically significant

Author Manuscript Author Manuscript Author Manuscript Author Manuscript

difference in the percentage of viable cells was observed among any of the test and control groups (Fig. 6).

These data suggest lupeol is not cytotoxic to HUVEC, corroborating the lack of systemic toxicity by lupeol *in vivo* [15] and the idea that lupane triterpenes is selectively cytotoxicity to highly proliferative tumor cells [19,20,41,42].

Accordingly, the Presto Blue cell viability assay suggested no statistically significantly difference between each lupeol treatment and EBM-2 10% FBS control over time. Additionally, two-way analysis of variance of lupeol curves of response suggest a statistically significant overall effect of treatment with lupeol, supporting the idea that it affects HUVEC proliferation.

Lupeol treatment decreases HUVEC migration, suggesting a putative role on its antiangiogenic properties. The observation of HUVEC response to lupeol exposure regarding the cell migration behavior, namely by analyzing remaining open area after treatment compared to the initial state, revealed statically significant decrease in HUVEC migration both on 30 μg/mL and 100 μg/mL lupeol concentrations when compared to EBM-2 10% FBS control (Fig. 7). These results suggest a more remarkable effect of lupeol on the migration component of angiogenesis promoted by HUVEC, on a way it presents antiangiogenic effects by impairing mechanisms related to cell migratory activity. Saleem et al. [39] observed lupeol modulates the expression of matrix metalloproteinases (MMPs), which might destroy components in the extracellular matrix important for adhesion, and consequently, migration. Additionally, lupeol was also shown to prevent the phosphorylation of cofilin, an actin-depolymerizing factor [43]. Finally, lupeol affects the motility and invasion of some cancer cell lines, but not others suggesting, again, significant differential effects depending on the cell type involved [43,44].

4.5. In vivo *antiangiogenic studies*

In order to confirm the lupeol antiangiogenic activity, the chorioallantoic membrane (CAM) model was applied. CAM assay is an *in vivo* model of angiogenesis originally developed for the study of embryonic tissues, and was adapted by Folkman in 1974 for the study of tumor angiogenesis, as well as for testing of pro and antiangiogenic substances. Currently, this model is also used for the evaluation of drug delivery systems, biomaterials, implants and tissue repair [45–49]. Lupeol treatment (100 μg/mL and 250 μg/ mL) promoted a reduction (39.41% and 44.12%, respectively) in the percentage of vessels compared with the control group (Fig. 8). The application of Bevacizumab (250 μg/mL) led to a reduction of 24.62% in the vessels, and it was significant different from the treatment with lupeol (250 μg/mL). These data suggest that lupeol treatment (250 μg/mL) was more efficient than bevacizumab, a drug with proven antiangiogenic activity being used in clinical practice for the treatment of cancer and proliferative eye diseases [50]. The topical application of PLGA ocular implants did not lead to a significant decrease of the vessels. However, the treatment carried out with PLGA ocular implants containing lupeol in concentration of 30% (w/w) resulted in a reduction of 30.77% in the vessels, similar to the results presented by bevacizumab.

Author Manuscript Author Manuscript Author Manuscript Author Manuscript

This study also investigated the biocompatibility of PLGA-lupeol implants (Fig. 8). The way in which CAM responds to the materials applied on its surface, with the presence of inflammation or neovascularization, is important for assessing the biocompatibility of topically applied drug delivery systems [51]. Application of the implants on the CAM did not lead to neovascularization, acute inflammatory response or vascular lysis, indicating the implants are biocompatible.

Ozurdex is a commercial polimeric implant based on the use of dexametazone drug. Ozurdex and Iluvien are intraocular polymer implants containing dexamethasone and fluocinolone acetonide, respectively, available for the treatment of macular edema. Bevacizumab is a monoclonal antibody and ranibizumab is a fragment of the antibody, with anti-VEGF activity that binds with high affinity to all isoforms of VEGF-A, the main class involved in pathogenic processes in the retina. They are administered by monthly intravitreal injection in the treatment of age-related macular degeneration (AMD) and have good efficacy; however, this route of administration is related to the occurrence of several adverse effects such as retinal detachment, cataract and endophthalmitis. Compared to them, the lupeol implant developed in this work may presents advantages such as the possibility of insertion into the vitreous cavity that increase the bioavailability of the drug in the retina and choroid, the biodegradability of the polymer matrix, and the prolonged release time, eliminating the need for repeated intravitreal injections and thereby reducing the adverse effects associated with them.

These results provide the rational and preliminary studies to further investigate the eye tolerance of the implants. Herein we showed that lupeol, as well as its PLGA delivery system, has a great potential for the treatment of diseases that cause retinal neovascularization due to biocompatibility and promising anti-angiogenic activity *in vivo*, assessed in the CAM assay and that are in agreement with *in vitro* tests.

5. Conclusion

Polymeric implants constituted by PLGA polymer and lupeol at 30% (w/w) were prepared and physicochemical characterized, revealing existing only physical interactions among its contents. These findings demonstrate that lupeol molecular structure was maintained unaltered in polymeric matrix and through normal biodegradation can be released without modifications. Although lupeol presents antitumor and antiangiogenic effects in different models, it is clear these effects do not necessarily derive from the modulation of the same cell processes. Pathways involved in processes such as cell survival, proliferation and migration may be differentially activated or repressed in distinct cell lines. Moreover, the cellular microenvironment (tissue or culture conditions) in addition to genetic predisposition, may play an important role in generating the heterogeneous results observed so far. Lupeol exhibits selective effects in human endothelial cells through its antiangiogenic activity, majorly by inhibiting cell migration, without significant effects on the viability of these non-tumor cells. Lupeol may be a promising compound for the treatment of angiogenesis-related diseases with reduced impact to healthy cells. These studies provided a promising and novel drug delivery platform for intravitreal administration, allowing a possible therapeutic option to treat diseases related to angiogenic process

Author Manuscript Author Manuscript Author Manuscript Author Manuscript

Supplementary Material

Refer to Web version on PubMed Central for supplementary material.

Acknowlegdments

The authors would like to thank CNPq (Conselho Nacional de Desenvolvimento Científico e Tecnológico) and FAPEMIG (Funda-ção de Amparo à Pesquisa do Estado de Minas Gerais) for their financial support.

References

[1]. Monteforte AJ, Lam B, Das S, Mukhopadhyay S, Wright CS, Martin PE, et al., Glypican-1 nanoliposomes for potentiating growth factor activity in therapeutic angiogenesis, Biomaterials 94 (2016)45–56, doi:10.1016/j.biomaterials.2016.03.048. [PubMed: 27101205]

[2]. Belair DG, Miller MJ, Wang S, Darjatmoko SR, Binder BYK, Sheibani N, et al., Differential regulation of angiogenesis using degradable VEGF-binding microspheres, Biomaterials 93 (2016) 27–37, doi:10.1016/j.biomaterials.2016.03.02. [PubMed: 27061268]

[3]. Kowluru RA, Mishra M, Kumar B, Diabetic retinopathy and transcriptional regulation of a small molecular weight G-Protein, Rac1, Exp. Eye Res 147 (2016) 72–77, doi:10.1016/j.exer. 2016.04.014. [PubMed: 27109029]

[4]. Ahmad S, El-Sherbiny NM, Jamal MS, Al-Zahrani FA, Haque R, Khan R, et al., Anti-inflammatory role of sesamin in STZ induced mice model of diabetic retinopathy, J. Neuroimmunol 295 (2016) 47–53, doi:10.1016/j.jneuroim.2016.04.002. [PubMed: 27235348]

[5]. Gillies MC, Campain A, Barthelmes D, Simpson JM, Arnold JJ, Guymer RH, et al., Long-term outcomes of treatment of neovascular age-related macular degeneration: data from an observational study, Ophthalmology 122 (2015) 1837–1845, doi:10.1016/j.ophtha.2015.05.010. [PubMed: 26096346]

[6]. Gopinath B, Liew G, Burlutsky G, Mitchell P, Age-related macular degeneration and risk of total and cause-specific mortality over 15 years, Maturitas 84 (2016) 63–67, doi:10.1016/j.maturitas. 2015.11.001. [PubMed: 26596903]

[7]. Teper SJ, Nowinska A, Pilat J, Wylegala E, Photodynamic therapy in VEGF inhibition non-responders-Pharmacogenetic study in age-related macular degeneration assessed with swept-source optical coherence tomography, Photodiagn. Photodyn. Ther 13 (2016) 108–113, doi: 10.1016/j.pdpdt.2016.01.006.

[8]. Bouraoui R, Bouladi M, Kort F, Limaiem R, Mghaieth F, El Matri L, Intravitreal bevacizumab in AMD complicated by submacular hemorrhage, J. Fr. D'ophtalmol 39 (2016) 248–254, doi: 10.1016/j.jfo.2015.10.010.

[9]. Wang D-D, Xu P-Y, Wang T-Y, Chen X-X, Peng Q, Observation on health quality of life before and after the injection of antiangiogenic drug in vitreous cavity to patients with wet age-related macular degeneration, Chin. Nurs. Res 2 (2015) 27–30, doi:10.1016/j.cnre.2015.07.001.

[10]. Douat J, Auriol S, Mahieu-Durringer L, Ancéle E, Pagot-Mathis V, Mathis A, Intravitreal bevacizumab for treatment of neovascular glaucoma. Report of20 cases, J. Fr. Déophtalmol 32 (2009) 652–663, doi:10.1016/j.jfo.2009.10.00.

[11]. Moon JS, Kim JH, Park IR, Lee JH, Kim HJ, Lee J, et al., Impaired RBC deformability is associated with diabetic retinopathy in patients with type 2 diabetes, Diabetes Metab. 42 (6) (2016) 448–452, doi:10.1016/j.diabet.2016.04.008. [PubMed: 27209441]

[12]. Boynton GE, Stem MS, Kwark L, Jackson GR, Farsiu S, Gardner TW, Multimodal characterization of proliferative diabetic retinopathy reveals alterations in outer retinal function and structure, Ophthalmology 122 (2015) 957–967, doi:10.1016/j.ophtha.2014.12.001. [PubMed: 25601533]

[13]. Jeon S, Lee WK, Intravitreal bevacizumab increases intraocular interleukin-6 levels at 1 day after injection in patients with proliferative diabetic retinopathy, Cytokine 60 (2012) 535–539, doi: 10.1016/j.cyto.2012.07.005. [PubMed: 22846147]

Author Manuscript Author Manuscript Author Manuscript Author Manuscript

[14]. Stitt AW, Curtis TM, Chen M, Medina RJ, McKay GJ, Jenkins A, et al., The progress in understanding and treatment of diabetic retinopathy, Prog. Retinal Eye Res 51 (2015) 156–186, doi:10.1016/j.preteyeres.2015.08.001.

[15]. Siddique HR, Saleem M, Beneficial health effects of lupeol triterpene: a review of preclinical studies, Life Sci. 88 (2011) 285–293, doi:10.1016/j.lfs.2010.11.020. [PubMed: 21118697]

[16]. de Andrade SF, Lemos M, Comunello E, Noldin VF, Filho VC, Niero R, Evaluation of the antiulcerogenic activity of Maytenus robusta (Celastraceae) in different experimental ulcer models, J. Ethnopharmacol 113 (2007) 252257, doi:10.1016/j.jep.2007.06.002.

[17]. Harish BG, Krishna V, Santosh Kumar HS, Khadeer Ahamed BM, Sharath R, Kumara Swamy HM, Wound healing activity and docking of glycogen- synthase-kinase-3-beta-protein with isolated triterpenoid lupeol in rats, Phytomedicine 15 (2008) 763–767, doi:10.1016/j.phymed.2007.11.017. [PubMed: 18222664]

[18]. Silva FC, Rodrigues VG, Duarte LP, Silva GDF, Miranda RRS, Filho SAV, A new friedelane triterpenoid from the branches of Maytenus gonoclada (Celastraceae), J. Chem. Res 35 (2011) 3, doi:10.3184/174751911X13161944590173.

[19]. You YJ, Nam NH, Kim Y, Bae KH, Ahn BZ, Antiangiogenic activity oflupeol from Bombax ceiba, Phyther. Res 17 (2003) 341–344, doi:10.1002/ptr.1140.

[20]. Laszczyk MN, Pentacyclic triterpenes of the lupane, oleanane and ursane group as tools in cancer therapy, Planta Med. 75 (2009) 1549–1560, doi:10.1055/s-0029-1186102. [PubMed: 19742422]

[21]. Sohn K-H, Lee H-Y, Chung H-Y, Young H-S, Yi S-Y, Kim K-W, Antiangiogenic activity of triterpene acids, Cancer Lett. 94 (1995) 213–218, doi: 10.1016/0304-3835(95)03856-R. [PubMed: 7543366]

[22]. Kiran MS, Viji RI, Sameer Kumar VB, Sudhakaran PR, Modulation of angiogenic factors by ursolic acid, Biochem. Biophys. Res. Commun 371 (2008) 556–560, doi:10.1016/j.bbrc.2008.04.108. [PubMed: 18448068]

[23]. Cárdenas C, Quesada AR, Medina MA, Effects of ursolic acid on different steps of the angiogenic process, Biochem. Biophys. Res. Commun 320 (2004) 402–408, doi:10.1016/j.bbrc.2004.05.183. [PubMed: 15219842]

[24]. Reichle ML, Complications of intravitreal steroid injections, Optometry 76 (2005) 450–460, doi:10.1016/j.optm.2005.06.013. [PubMed: 16150412]

[25]. Cho HJ, Yoo SG, Kim HS, Kim JH, Kim CG, Lee TG, et al., Risk factors for geographic atrophy after intravitreal ranibizumab injections for retinal angiomatous proliferation, Am.J. Ophthalmol 159 (2015) 285–292, doi:10.1016/j.ajo.2014.10.035e. [PubMed: 25447115]

[26]. Salunkhe AB, Khot VM, Pawar SH, Magnetic hyperthermia with magnetic nanoparticles: a status review, Curr. Top. Med. Chem 14 (5) (2014) 572–594 http://www.ncbi.nlm.nih.gov/pubmed/24444167. (Accessed 12 February 2014). [PubMed: 24444167]

[27]. Kitagawa Y, Shimada H, Mori R, Tanaka K, Yuzawa M, Intravitreal tissue plasminogen activator, ranibizumab, and gas injection for submacular hemorrhage in polypoidal choroidal vasculopathy, Ophthalmology 123 (2016) 1278–1286, doi:10.1016/j.ophtha.2016.01.035. [PubMed: 26949121]

[28]. Fialho SL, Behar-Cohen F, Silva-Cunha A, Dexamethasone-loaded poly (epsilon-caprolactone) intravitreal implants: a pilot study, Eur. J. Pharm. Biopharm 68 (2008) 637–646, doi:10.1016/j.ejpb.2007.08.004. [PubMed: 17851057]

[29]. Kiddee W, Trope GE, Sheng L, Beltran-Agullo L, Smith M, Strungaru MH, et al., Intraocular pressure monitoring post intravitreal steroids: a systematic review, Surv. Ophthalmol 58 (2013) 291–310, doi:10.1016/j.survophthal.2012.08.003. [PubMed: 23768920]

[30]. Choonara YE, Pillay V, Danckwerts MP, Carmichael TR, du Toit LC, A review of implantable intravitreal drug delivery technologies for the treatment of posterior segment eye diseases, J. Pharm. Sci 99 (2010) 2219–2239, doi:10.1002/jps.21987. [PubMed: 19894268]

[31]. Yasin MN, Svirskis D, Seyfoddin A, Rupenthal ID, Implants for drug delivery to the posterior segment of the eye: a focus on stimuli-responsive and tunable release systems, J. Control. Release 196 (2014) 208–221, doi:10.1016/j.jconrel.2014.09.030. [PubMed: 25307997]

[32]. Fialho SL, da Silva Cunha A, Manufacturing techniques of biodegradable implants intended for intraocular application., Drug Deliv. 12 (n.d.) 109–116. 2005 doi:10.1080/10717540590921432. [PubMed: 15824036]

Author Manuscript Author Manuscript Author Manuscript Author Manuscript

[33]. Barcelos LS, Duplaa C, Kränkel N, Graiani G, Invernici G, Katare R, et al., Human CD133+ progenitor cells promote the healing of diabetic ischemic ulcers by paracrine stimulation of angiogenesis and activation of Wnt signaling, Circ. Res 104 (2009).

[34]. Kundu AP, 13C Nmr spectra of pentacyclic triterpenoids-a and some salient features, Phytochemistry 37 (1994) 1517–1575, doi:10.1016/S0031-9422(00)89569-2.

[35]. Macedo RO, Barbosa-Filho JM, da Costa EM, de Souza AG, Thermal Behaviour of some terpenoids, J. Therm. Anal. Calorim 56 (1999) 1353–1357.

[36]. Mainardes RM, Gremião MPD, Evangelista RC, Thermoanalytical study of praziquantel-loaded PLGA nanoparticles, Rev. Bras. Ciencias Farm 42 (2006) 523–530, doi:10.1590/S1516-93322006000400000.

[37]. Yang J, Lee C-H, Park J, Seo S, Lim E-K, Song YJ, et al., Antibody conjugated magnetic PLGA nanoparticles for diagnosis and treatment of breast cancer, J. Mater. Chem 17 (2007) 2695, doi:10.1039/b702538f.

[38]. Mitra SK, Mikolon D, Molina JE, Hsia DA, Hanson DA, Chi A, et al., Intrinsic FAK activity and Y925 phosphorylation facilitate an angiogenic switch in tumors, Oncogene 25 (2006) 5969–5984, doi:10.1038/sj.onc.1209588. [PubMed: 16682956]

[39]. Saleem M, Murtaza I, Tarapore RS, Suh Y, Adhami VM, Johnson JJ, et al., Lupeol inhibits proliferation ofhuman prostate cancer cells by targeting beta- catenin signaling, Carcinogenesis 30 (2009) 808–817, doi:10.1093/carcin/bgp044. [PubMed: 19233958]

[40]. Ambasta RK, Jha SK, Kumar D, Sharma R, Jha NK, Kumar P, Comparative study of anti-angiogenic activities of luteolin, lectin and lupeol biomolecules, J. Transl. Med 13 (2015) 307, doi:10.1186/s12967-015-0665-z. [PubMed: 26385094]

[41]. Liu F, He Y, Liang Y, Wen L, Zhu Y, Wu Y, et al., PI3-kinase inhibition synergistically promoted the anti-tumor effect of lupeol in hepatocellular carcinoma, Cancer Cell Int. 13 (2013) 108, doi:10.1186/1475-2867-13-108. [PubMed: 24176221]

[42]. Xiao X, Wang W, Liu D, Zhang H, Gao P, Geng L, et al., The promotion of angiogenesis induced by three-dimensional porous beta-tricalcium phosphate scaffold with different interconnection sizes via activation of PI3K/Akt pathways, Sci. Rep 5 (2015) 9409, doi:10.1038/srep09409. [PubMed: 25797242]

[43]. Hata K, Hori K, Murata J, Takahashi S, Remodeling of actin cytoskeleton in lupeol-induced B16 2F2 cell differentiation, J. Biochem 138 (2005) 467–472, doi:10.1093/jb/mvi15. [PubMed: 16272141]

[44]. Siveen KS, Nguyen AH, Lee JH, Li F, Singh SS, Kumar AP, et al., Negative regulation of signal transducer and activator of transcription-3 signalling cascade by lupeol inhibits growth and induces apoptosis in hepatocellular carcinoma cells, Br. J. Cancer 111 (2014) 1327–1337, doi:10.1038/bjc.2014.422. [PubMed: 25101566]

[45]. Auerbach R, Lewis R, Shinners B, Kubai L, Akhtar N, Angiogenesis assays: a critical overview, Clin. Chem 49 (2003) 32–40. [PubMed: 12507958]

[46]. Seidlitz E, Korbie D, Marien L, Richardson M, Singh G, Quantification of antiangiogenesis using the capillaries of the chick chorioallantoic membrane demonstrates that the effect of human angiostatin is age-dependent, Microvasc. Res 67 (2004) 105–116. [PubMed: 15020201]

[47]. Vargas A, Zeisser-Labouébe M, Lange N, Gurny R, Delie F, The chick embryo and its chorioallantoic membrane (CAM) for the in vivo evaluation of drug delivery systems, Adv. Drug Deliv. Rev 59 (2007) 1162–1176. [PubMed: 17870202]

[48]. Ribatti D, The chick embryo chorioallantoic membrane in the study of tumor angiogenesis, Rom. J. Morphol. Embryol 49 (2008) 131–135. [PubMed: 18516317]

[49]. Nowak-Sliwinska P, Ballini J-P, Wagniéres G, van den Bergh H, Processing of fluorescence angiograms for the quantification of vascular effects induced by anti-angiogenic agents in the CAM model, Microvasc. Res 79 (2010) 21–28. [PubMed: 19857502]

[50]. Klein A, Loewenstein A, Therapeutic monoclonal antibodies and fragments: bevacizumab, Dev. Ophthalmol 55 (2016) 232–245, doi:10.1159/000431199. [PubMed: 26502311]

[51]. Valdes TI, Kreutzer D, Moussy F, The chick chorioallantoic membrane as a novel in vivo model for the testing of biomaterials, J. Biomed. Mater. Res 62 (2002) 273–282, doi:10.1002/jbm.10152. [PubMed: 12209948]

Author Manuscript Author Manuscript Author Manuscript Author Manuscript

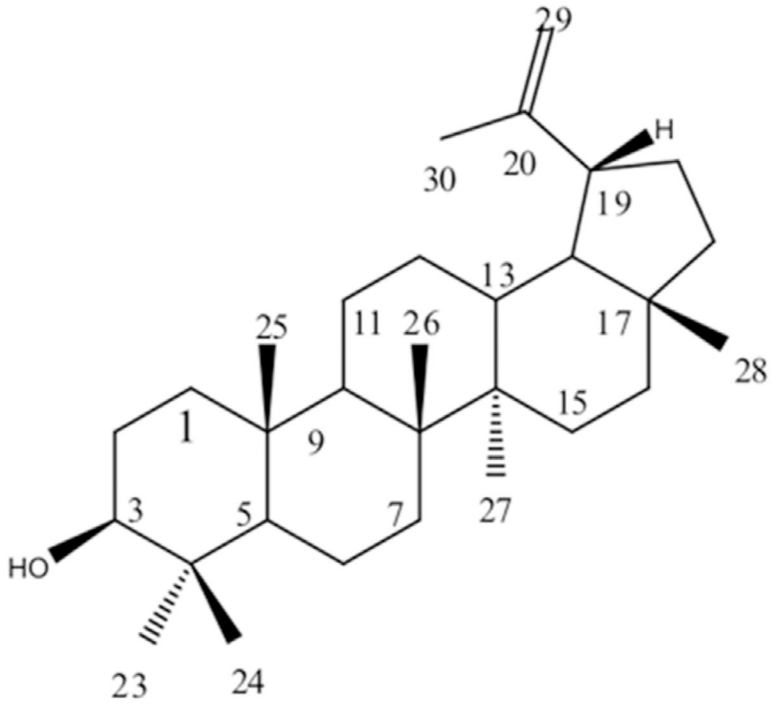

Fig. 1.
Lupeol. Molecular formula: $C_{30}H_{50}O$. Molecular mass: 426 g/mol.

Author Manuscript Author Manuscript Author Manuscript Author Manuscript

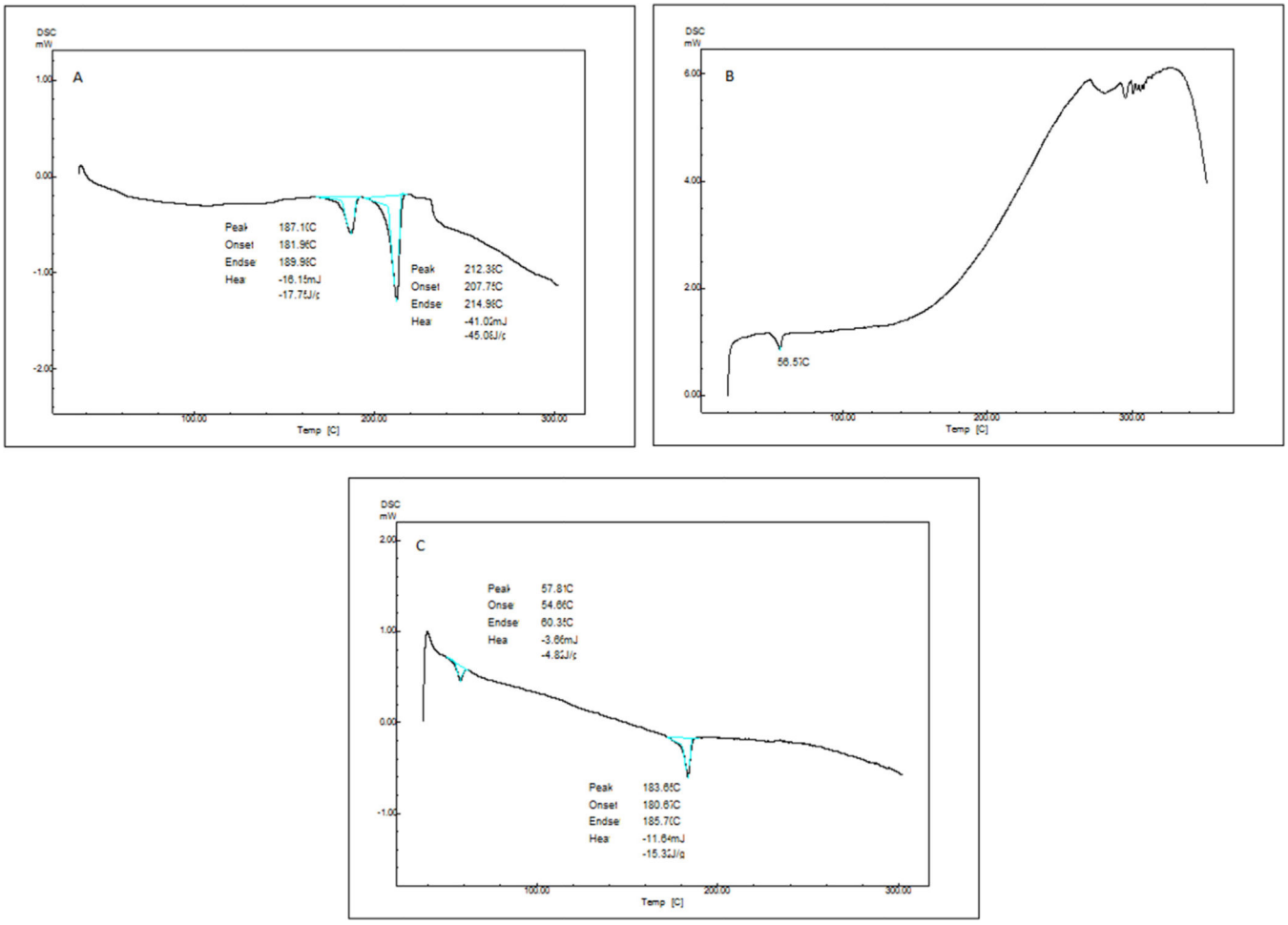

Fig. 2.

Differential Scanning Calorimetry analysis (DSC) of (A) Lupeol; (B) Blank PLGA 75:25 and (C) lupeol-loaded PLGA ocular implants. Samples were heated in semi-hermetic aluminum pans, and the first scan was measured at a heating rate of 10 °C min^{-1} from room temperature to 180 °C. Subsequently, the samples were cooled to −100 °C and heated to 400 °C (second run) under nitrogen atmosphere.

Author Manuscript Author Manuscript Author Manuscript Author Manuscript

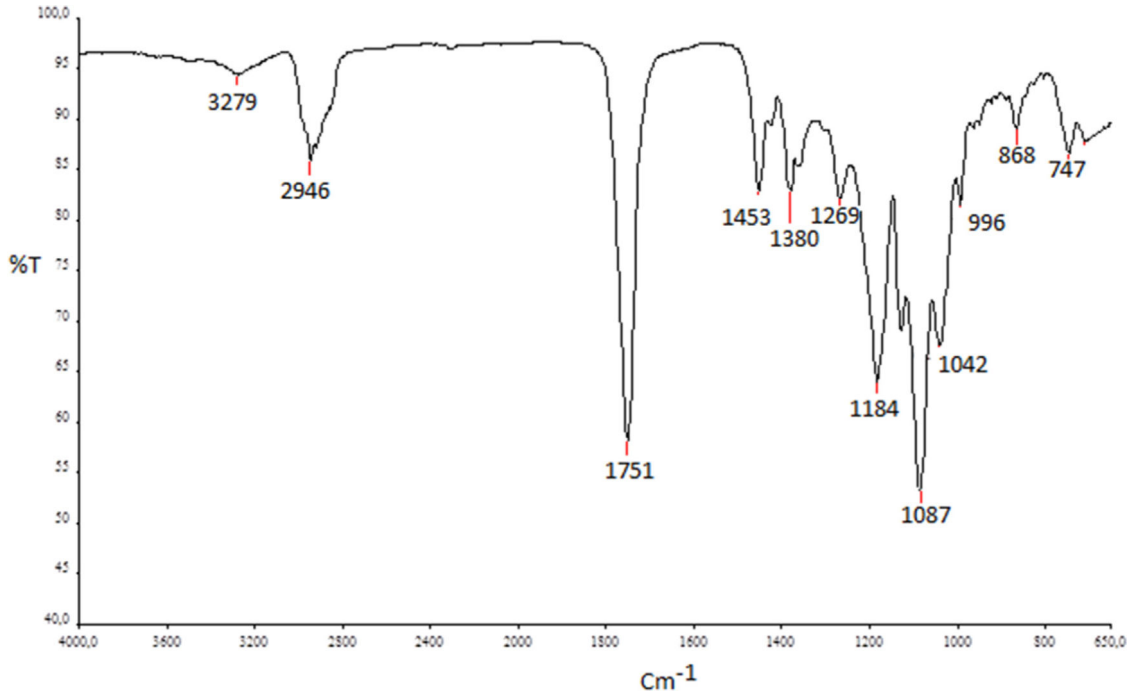

Fig. 3.

Lupeol-loaded PLGA ocular implants FTIR spectrum. Samples were evaluated using the attenuated total reflectance (ATR) technique. Each spectrum was a result of 32 scans with a resolution of 4 cm^{-1}, between ranging 4000–650 cm^{-1}.

Author Manuscript Author Manuscript Author Manuscript Author Manuscript

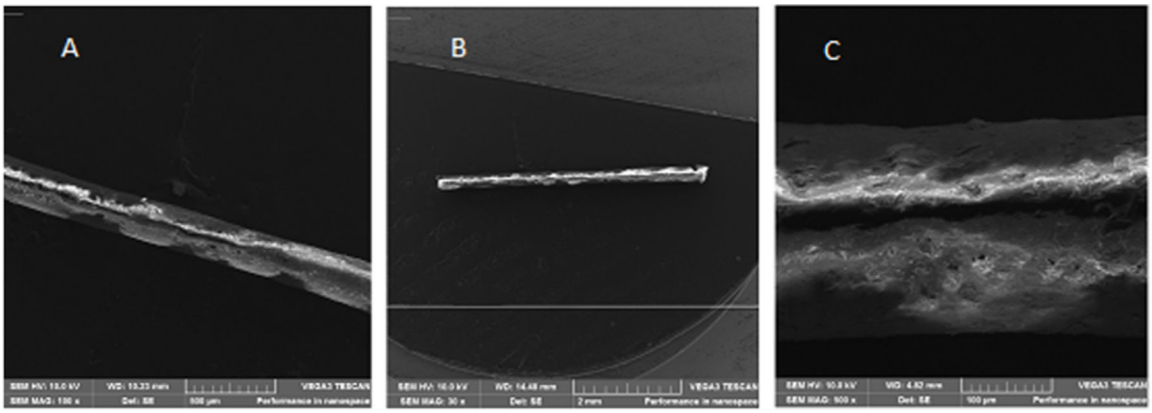

Fig. 4.

Lupeol-loaded PLGA ocular implants SEM images. Magnification of (a) 100× (b) 30× and (c) of 500×.

Author Manuscript Author Manuscript Author Manuscript Author Manuscript

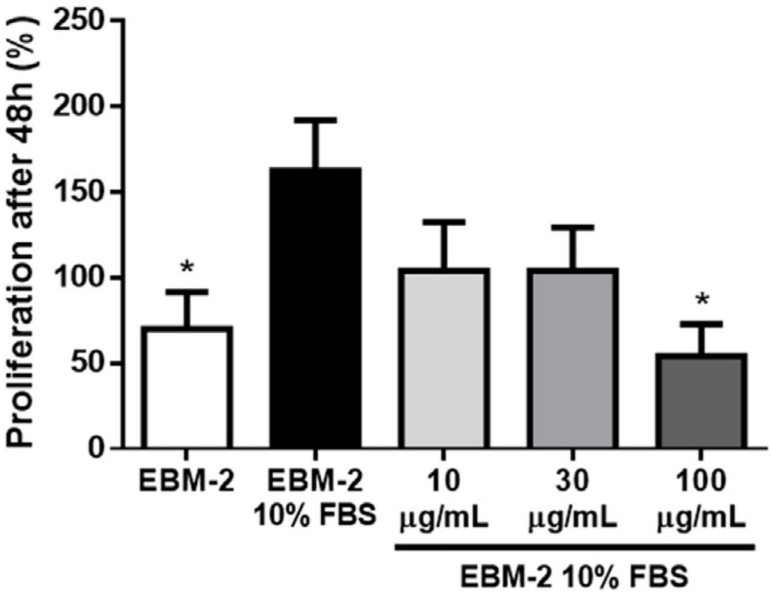

Fig. 5.

Effect of Lupeol on endothelial cell proliferation. HUVEC were cultured during 48 h in the presence or absence of Lupeol. We observed a decrease in the proliferation rate only in the presence of 100 µg/mL lupeol when compared to the Endothelial Basal Medium (EBM-2) 10% FBS control group. Results are expressed as mean ± SEM; * $p < 0.05$ compared to EBM-2 10% FBS.

Author Manuscript Author Manuscript Author Manuscript Author Manuscript

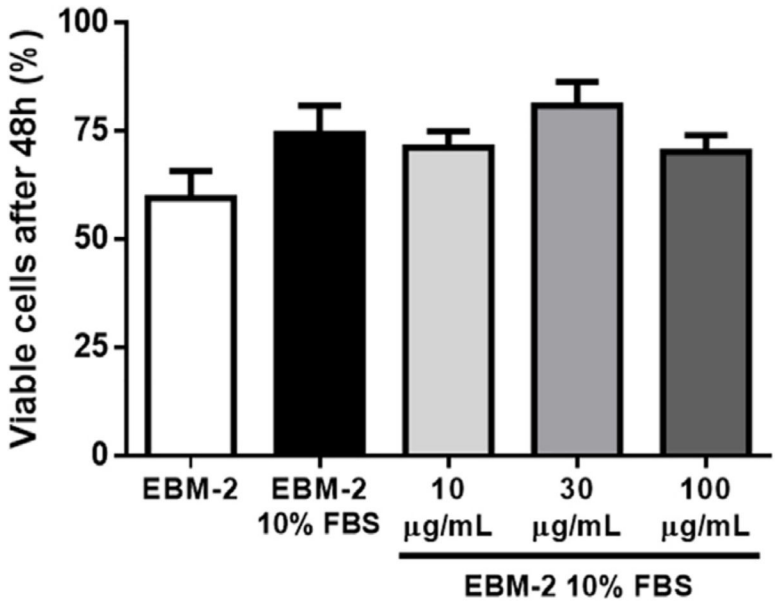

Fig. 6.

Effect of Lupeol on HUVEC viability. Cell viability was measured using the Trypan Blue assay. No statistically significant difference in the percentage of viable cells was observed among any of the test and control groups.

Author Manuscript Author Manuscript Author Manuscript Author Manuscript

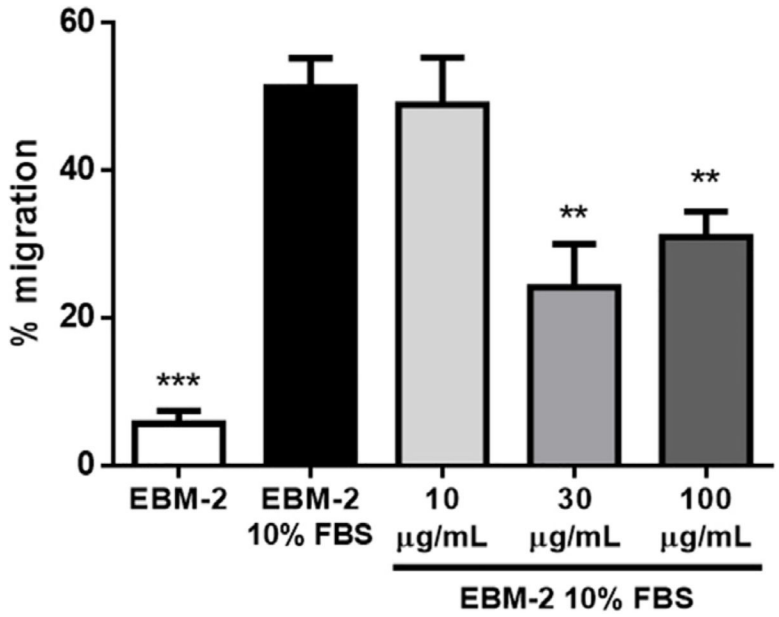

Fig. 7.

Effect of lupeol on endothelial cell migration. HUVEC were incubated for 36 h after scratching in the presence or absence of lupeol. We observed a decrease in the gap closure rate (namely the remaining gap area after treatment compared to the initial gap) in the presence of both 30 µg/mL and 100 µg/mL lupeol when compared to the EBM-2 10% FBS control group. Results are expressed as mean ± SEM; ** $p < 0.01$ and *** $p < 0.001$ compared to EBM-2 10% FBS.

Author Manuscript Author Manuscript Author Manuscript Author Manuscript

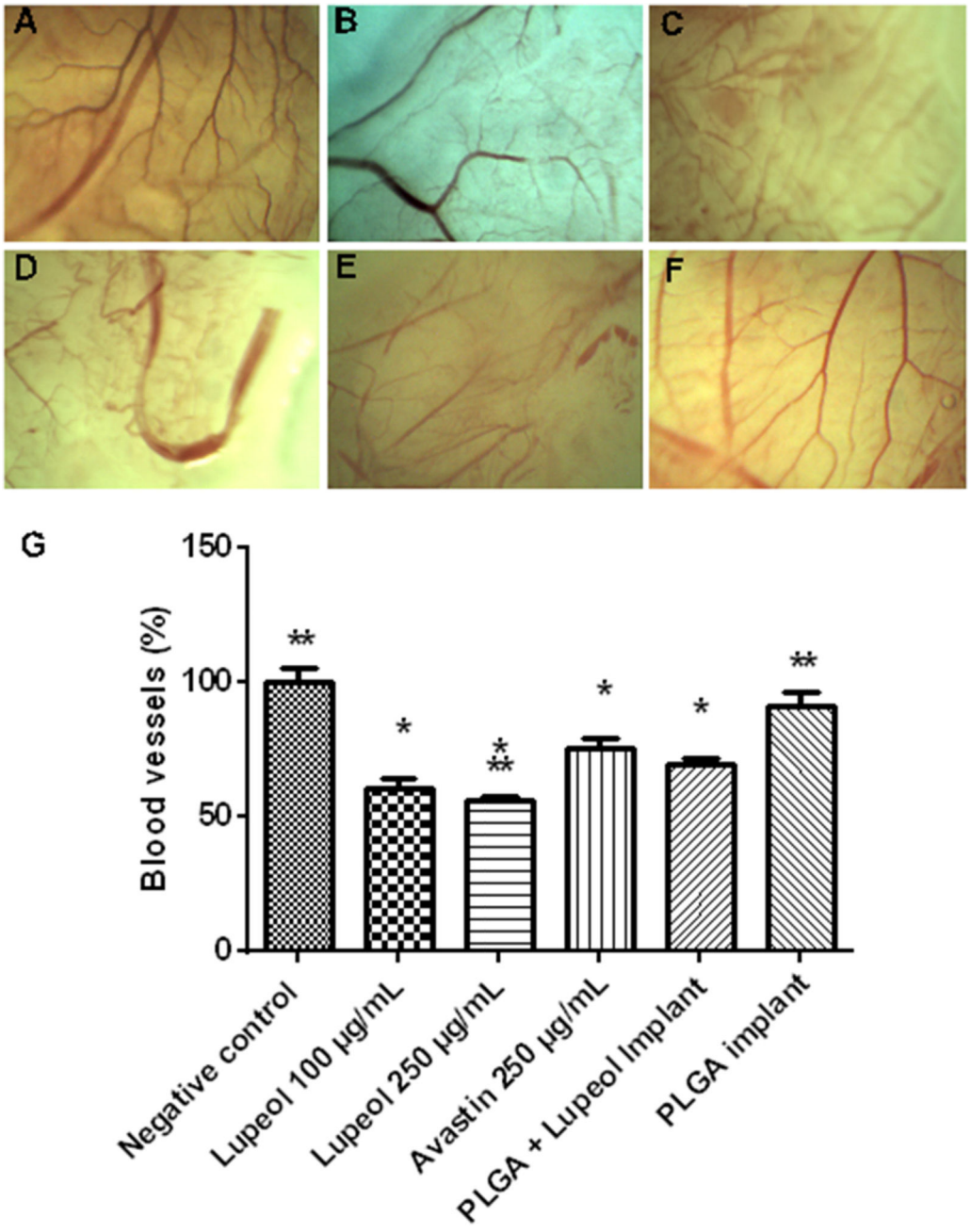

Fig. 8.

Chorioallantoic membrane assay performed with: (A) PBS (negative control); (B) bevacizumab 250 µg/mL (positive control); (C) lupeol 250 µg/mL; (D) lupeol 100 µg/mL; (E) PLGA implant containing lupeol; (F) PLGA implant. The percentage of blood vessels on the treated group was expressed in relation to the percentage of the negative control group fixed at 100% (G). * Significantly different from the negative control group. ** Significantly different from the group treated with bevacizumab (250 µg/mL) ($P < 0.05$).